Surrogate-based aerodynamic optimization of proprotor blades for a parcel delivery UAV

Sooin PARK[1], Usama YOUNUS*,[2]

*Corresponding author
[1]Plamica Labs,
Battan Hall, 125 Western Ave, Allston, MA 02173, USA,
sooin.park@plamica.com
*,[2]Department of Computer Science, University of Maryland, College Park,
150 Brendan Iribe Center, 8125 Paint Branch Drive, College Park, MD 20742, USA,
uyounus@umd.edu

DOI: 10.13111/2066-8201.2025.17.3.4

Received: 24 July 2025/ Accepted: 24 August 2025/ Published: September 2025

Abstract: *This study presents a surrogate-based aerodynamic optimization framework for a quad-tiltrotor platform designed for both hover and forward flight. To obtain an optimized blade design in both hover and forward flight conditions, a free wake model is coupled with Gaussian Process Regression (GPR). The framework enables efficient exploration of the design space while maintaining physical fidelity in rotor modeling. The rotor blade geometry is parameterized using piecewise linear functions for twist and taper distributions, allowing localized shape control during optimization. Latin Hypercube Sampling (LHS) is used to generate initial design points, and the surrogate model is iteratively refined using the Expected Improvement criterion. The final optimized blade exhibits a 3.7% improvement in hover figure of merit and a 38.3% increase in cruise propulsive efficiency compared to the baseline blade. These gains result from redistributed twist and chord distributions that enhance spanwise loading and reduce induced power loss. The results demonstrate the efficacy of combining free wake analysis with surrogate modeling for the design of UAV-scale rotorcraft.*

Key Words: *Unmanned Aerial Vehicle (UAV), Blade Design Optimization, Gaussian Process Regression (GPR), Proprotor Design, Surrogate-Based Optimization*

1. INTRODUCTION

Unmanned Aerial Vehicles (UAVs) are experiencing rapid technological advances and deployment in a variety of civil and commercial applications, including surveillance, agriculture, inspection, and logistics [1–3]. Among these, last-mile parcel delivery has emerged as a major driver of innovation, driven by the need for on-demand, efficient, and contactless transportation solutions. Companies such as Amazon Prime Air, Alphabet's Wing, UPS Flight Forward, and Zipline are actively developing or operating UAV-based logistics systems to serve urban and rural customers, and such a logistics system requires a UAV platform with high maneuverability and an extended flight range.

Traditional multirotor drones are well suited for vertical takeoff and landing (VTOL), enabling deployment in confined environments. However, their limited endurance and low aerodynamic efficiency in forward flight inhibit their use in long-range networks. Conversely,

fixed-wing UAVs have greater range and superior cruise performance, but they necessitate runways or launch infrastructure, hence constraining their adaptability in densely populated urban environments. To address this operational gap, a hybrid system featuring tilting rotors, known as proprotor UAVs, have gained significant attention [4]. These configurations enable a seamless transition between hover and forward flight, combining the advantages of rotary and fixed-wing aircraft within a single platform. As a result, proprotor UAVs are emerging as a promising solution for automated delivery networks that require both point-to-point accessibility and energy efficient cruise.

To fully exploit the aerodynamic versatility of such a platform, rotor blade design becomes a critical factor, particularly in achieving high thrust-to-power ratio during hover and minimizing drag in cruise. The requirement of hover and forward flight mode presents a complex optimization challenge of a wide range of flight conditions and operating regimes. In large-scale rotorcraft, the blade optimization has been thoroughly examined using analytical, empirical, and high-fidelity computer methods [5, 6]. These methods have led to significant improvements in rotor performance, reduced vibration, and enhanced noise suppression. However, the optimization research for UAV scale proprotors is limited. Given the increasing operational complexity and performance expectations for UAV, there is a growing need for systematic, mission-oriented blade optimization methodologies of UAV-scale rotors.

The aerodynamic performance of rotor blades is influenced by complicated aerodynamic interactions, including variable inflow distributions, blade wake interaction (BWI), and stall dynamics. The significance of these effects is particularly pronounced in tiltrotor systems where blade loading and inflow conditions vary markedly between hover and cruise [7]. Consequently, the rotor design problem is highly multi-objective and requires global optimization strategies to search for effective solutions. However, global search techniques, such as evolutionary algorithms, when coupled with high-fidelity solvers like CFD, can be computationally expensive and often impractical for iterative design workflows [8]. To overcome this challenge, a mid-fidelity aerodynamic model, such as the free wake method, is widely used to efficiently optimize the blade planform with understandable accuracy. Unlike prescribed wake models, which assume the wake geometry is prescribed, free wake formulations dynamically resolve wake geometry and interactions, allowing an accurate prediction of induced velocities and rotor performance under unstable conditions [9]. Free wake simulations are adopted into several research studies [10–12], and the results show their potential to capture key performance characteristics while maintaining computational efficiency.

As a global optimizer, the use of surrogate models such as Gaussian Process Regression (GPR) models has gained popularity to accelerate design optimization. GPR enables fast prediction of blade performance in the design space while quantifying uncertainty, making it well suited for global search methods such as Efficient Global Optimization (EGO) [13]. Building upon these foundations, the present study proposes a surrogate-based aerodynamic optimization framework for proprotor blades of UAV-scale platforms. The framework adopts an aerodynamic solver with free wake method and an optimizer with GPR-based surrogate model to find the global optimum solution that balances hover and cruise efficiency.

2. METHODOLOGY

The Quad Tiltprop-UAV(QTP-UAV), developed by the Korea Aerospace Research Institute (KARI), is a quad-tiltrotor UAV designed for vertical takeoff and landing (VTOL) and efficient forward flight [14]. Each of the 4 tilting rotors is equipped and capable of tilting for

a smooth transition between hover and cruise modes. This hybrid capability makes it a promising candidate for autonomous parcel delivery missions.

Fig. 1 – Image of the QTP-UAV

The QTP-UAV is a 50 kg-class quad tiltrotor UAV platform designed to combine the advantages of rotary-wing and fixed-wing configurations. The vehicle is equipped with four rotatable prop-rotors and driven by a hybrid propulsion system (internal combustion engine + electric battery). Each rotor has three blades operating under differential tilt angles for hover and forward flight. Key flight specifications are summarized in Table 1. The vehicle is capable of carrying a 3.0 kg of payload and hovering for up to 15 minutes. The maximum speed of the aircraft is 180 km/h with maximum endurance of 2 hours.

Table 1 – Specifications of QTP-UAV

Specification	**Value**
Gross Weight	48.0 kg
Payload	3.0 kg
Max. Speed	180 km/h
Hover Endurance	15 min
Max. Endurance	2 hours
Number of Prop-rotors	4
Number of blades per rotor	3
Prop-rotor Radius	0.55 m

A. Aerodynamic analysis with free wake model

To analyze rotor aerodynamics, this study employs a blade element theory (BET) coupled with a free wake model. In this formulation, each rotor blade is modeled as a lifting line and discretized into multiple spanwise elements. The aerodynamic loads on each element are then calculated using local inflow velocity, which is not prescribed but computed from the induced velocity field generated by the rotor wake itself. To capture this induced inflow accurately, a free wake model is used. The free wake model represents the rotor wake as a collection of

discrete vortex filaments that are shed from the blade trailing edges and convected downstream under the influence of both self-induced and freestream velocities. Unlike prescribed wake models, which impose fixed wake geometries, the free wake method allows the wake to deform and evolve dynamically according to the flow field, providing a more realistic representation of rotor–wake and wake–wake interactions [15], which can be represented as:

$$v_{ind}(x) = \frac{\Gamma}{4\pi} \int \left[\frac{r \times dl}{|r|^3} \right] \tag{1}$$

where $r = x - x'$ is the position vector from the vortex segment element to the field point, and dl is the differential length vector along the filament.
The motion of the wake filaments is governed by:

$$\frac{dx}{dt} = v_{ind}(x) + v_{free} \tag{2}$$

where v_{free} is the freestream or forward flight velocity. Each time step updates the wake geometry iteratively to reflect the influence of wake–wake and blade–wake interactions.

To verify the fidelity of the implemented free wake model, hover performance of the QTP-UAV rotor was simulated and compared against validated reference data from Ref. [14], as illustrated in Fig. 2. The thrust–power characteristics predicted by the present model show good agreement with the reference results across a wide range of thrust conditions. Specifically, the predicted power consumption at the operational thrust level of 139.3N closely aligns with the data from Ref. [14], indicating accurate capture of induced velocity and wake evolution. This result demonstrates that the current free wake formulation can reliably predict the performance of the QTP-UAV without validating its applicability as an analysis tool for subsequent surrogate model training and design optimization.

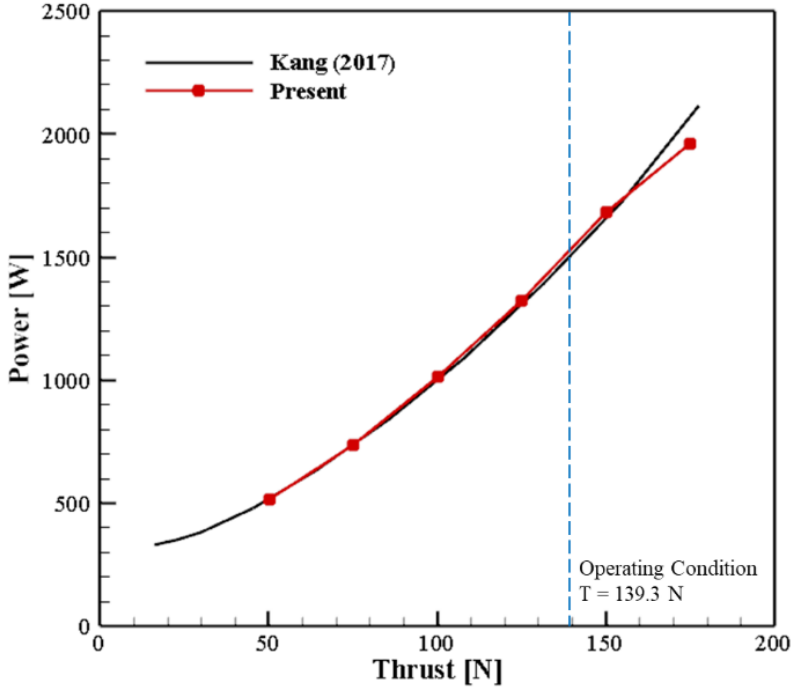

Fig. 2 – Validation of free wake model in hover flight

B. Gaussian Process Regression (GPR) for surrogate modeling

Gaussian Process Regression (GPR) is employed in this study to construct a surrogate model of rotor performance based on high-fidelity simulation data. GPR is a probabilistic machine learning method that offers both mean predictions and uncertainty estimates, making it highly suitable for design optimization and adaptive sampling. Instead of assuming a specific functional form, GPR models the output as a distribution over functions, defined by a mean function $\mu(x)$ and a covariance (kernel) function $k(x, x')$:

$$Y(x) \sim GP(\mu(x), k(x, x')) \tag{3}$$

where x represents the vector of design variables.

For the kernel function which encodes assumptions about the smoothness and correlation structure of the target function, a widely used choice is the squared exponential (or radial basis function) kernel:

$$k(x, x') = \sigma_f^2 \times exp[-0.5 * (x - x')^T * L^{-1} * (x - x')] \tag{4}$$

where σ_f^2 is the signal variance representing output scale, and $L = diag(l_1^2, \dots, l_d^2)$ is a diagonal matrix of length-scale parameters for each input dimension, controlling the sensitivity to input variation.

These hyperparameters are typically estimated by maximizing the marginal likelihood of the observed data. Given training data $\{X, y\}$, where $X = [x_1, x_2, \dots, x_n]$ are the input samples and y is the corresponding vector of simulation outputs, the predictive distribution at a new point x^* is Gaussian with the following closed-form expressions for the posterior mean and variance:

$$\mu_* = k_*^T \times (K + \sigma_n^2 I)^{-1} \times y \tag{5}$$

Here, K is the kernel matrix $n \times n$ evaluated between all training inputs, k_* is the vector of kernel values between the test point x^* and the training points X, and σ_n^2 is the variance in noise, accounting for the uncertainty of the model or the simulation error. The strength of GPR lies in its ability to provide not only predictions, but also uncertainty estimates that vary across the design space. If some regions are densely populated with training data, the predicted variance is low, reflecting high model confidence while in unexplored regions, the predicted variance is high, stimulating the need to update the model in those regions.

In this study, the GPR model is trained with simulation outputs from a free wake aerodynamic solver, including performance metrics such as figure of merit and propulsive efficiency. Once trained, the surrogate model can be used to efficiently evaluate rotor performance enabling rapid exploration of trade-offs between hover and cruise performance in the tiltrotor blade design.

C. Proprotor optimization framework

The optimization framework for QTP-UAV prop-rotor blade design consists of a structured integration of sampling, surrogate modeling, and performance prediction. The objective is to maximize aerodynamic efficiency in both hover and forward flight while reducing computational cost. The process begins with the generation of an initial set of design samples using the Latin Hypercube Sampling (LHS) method, which ensures an uniform and comprehensive distribution across the multi-dimensional design space, providing an efficient basis for training. Each sampled design is evaluated through high-fidelity aerodynamic

simulations using a free wake model to obtain performance metrics such as thrust, torque, power, figure of merit, and propulsive efficiency. These results form the initial dataset for training a Gaussian Process Regression (GPR) surrogate model. To guide the iterative refinement of the surrogate model, new design points are selected using the Expected Improvement (EI) acquisition function. EI quantitatively reconciles the exploitation of high-performing regions with exploration of doubtful areas by incorporating both the predicted mean and variance of the GPR model. Specifically, higher EI values occur in regions characterized by low predicted objective values or high uncertainty, making EI an effective metric for navigating complex design spaces. This strategy allows the optimizer to actively explore under-sampled regions where significant improvements may be found, enabling efficient global optimization. Consequently, the GPR model becomes progressively more accurate in critical regions of the design space, leading to faster convergence toward an optimal prop-rotor blade configuration.

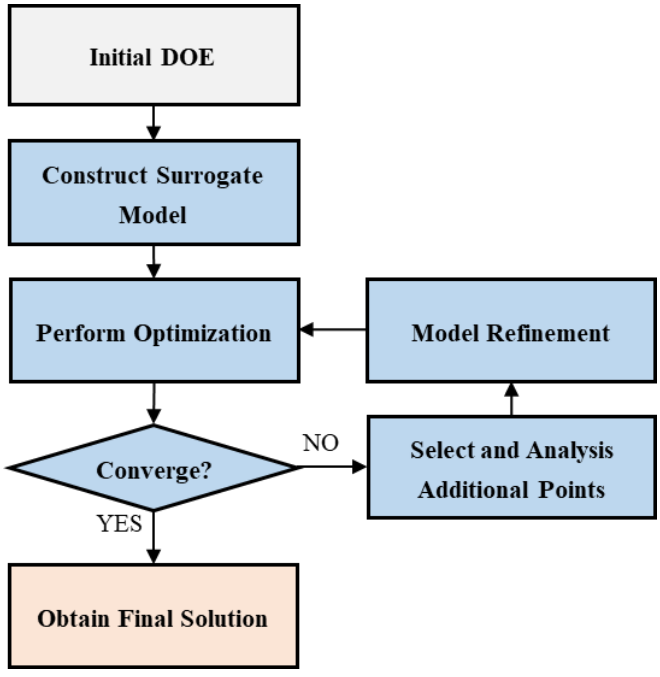

Fig. 3 – Proprotor optimization framework for QTP-UAV blade design

The Expected Improvement criterion is defined as follows:

$$EI = (f_{min} - \hat{y})\Phi\left(\frac{f_{min} - \hat{y}}{s}\right) + s\phi\left(\frac{f_{min} - \hat{y}}{s}\right) \quad (6)$$

Once the surrogate model is sufficiently refined through iterative sampling and model updates, a final global optimization is performed over the surrogate to identify the optimal design configuration. This step exploits the high accuracy of the trained surrogate in regions of interest to efficiently search for the best-performing solution. The resulting optimal blade geometry satisfies the multi-objective design criteria—namely, maximizing aerodynamic efficiency in both hover and forward flight modes—while significantly reducing the computational cost compared to a purely simulation-driven approach. The final optimal solution is then verified through additional high-fidelity simulations to confirm its performance and consistency with the surrogate prediction.

3. RESULTS

The primary goal of the rotor blade optimization is to enhance aerodynamic efficiency across both hover and forward flight conditions. This multi objective requirement arises from the mission profile of the QTP-UAV platform, which demands vertical takeoff and landing capability as well as efficient long-range cruise flight. Accordingly, two performance metrics are defined: the figure of merit (FM) for hover efficiency, and the advance ratio J as a proxy for propulsive efficiency in forward flight.

$$Maximize: FM(hover),\ J(forward\ flight) \tag{7}$$

The FM is calculated as the ratio of ideal to actual power required in hover, while $J = V/(nD)$ is used to quantify thrust-to-power efficiency in axial flight, where V is the freestream velocity, n is the rotation frequency, and D is the rotor diameter.

To reflect real operational constraints, the flight conditions for both regimes are selected based on mission-specific performance targets of the QTP-UAV. These include realistic altitude, speed, and rotor speed conditions for both hover and cruise. Table 2 summarizes the representative operating points used during optimization.

Table 2 – Operating Conditions for Optimization

Hover Mode	
Environment	*ISA*
Altitude	*0 m*
Rotational Speed	*1800 RPM*
Required Thrust	*139.3 N*
Tilt Angle	*90 deg*
Forward Flight Mode	
Environment	*ISA*
Altitude	*1000 m*
Rotational Speed	*1800 RPM*
Required Thrust	*13 N*
Tilt Angle	*0 deg*
Flight Speed	*150 km/h*
Angle of Attack	*5.2 deg*

These conditions are selected to reflect typical delivery mission profiles in both urban hover operations and rural cruise segments. The tilt angles (90 degree for hover, 0 degree for forward flight) correspond to the full tiltrotor transition range, ensuring the final design is robust across extreme flight modes.

The blade geometry is parameterized using a flexible piecewise-linear scheme, which allows sufficient geometric adaptability while maintaining smooth aerodynamic shapes. As shown in Fig. 4, both the twist and taper (chord) distributions are segmented into three linear

regions, separated by two internal control points. This parameterization enables local refinement of blade shaping, which is particularly beneficial for managing the trade-off between hover and cruise requirements.

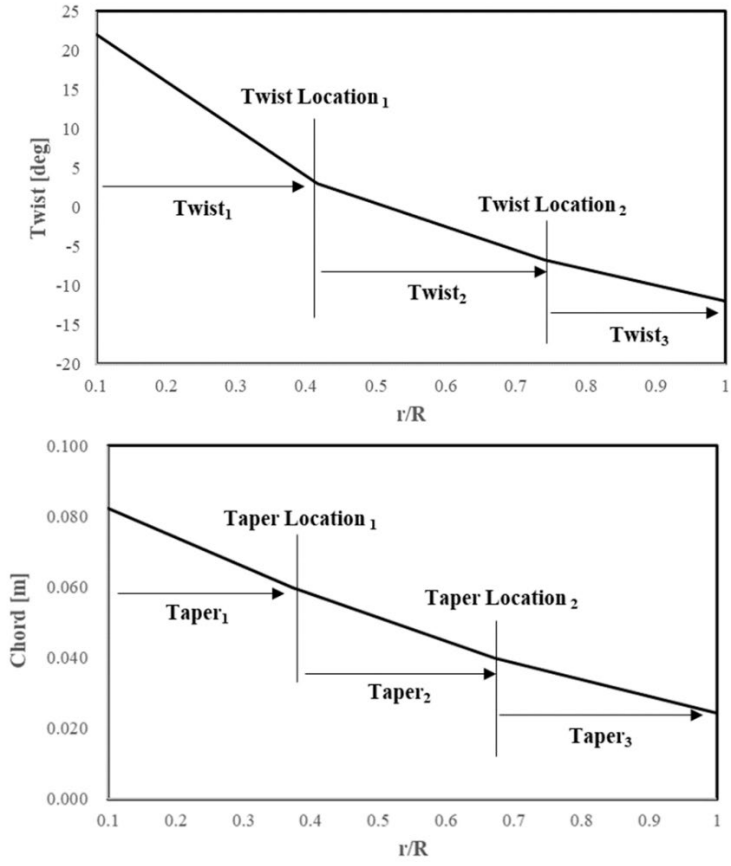

Fig. 4 – Definition of twist (left) and taper (right) distributions for parameterization

Each twist segment controls the blade angle along a specific radial span, providing control over inflow angle and angle of attack distribution. Similarly, the taper segments define chord contraction, which affects both lift production and blade drag distribution. The use of three-segment control enables localized shaping without excessive design freedom, maintaining numerical robustness during optimization.

The design variable bounds are defined to allow both aggressive and conservative shaping, encompassing a wide range of potential rotor configurations. Table 3 summarizes the design space explored during optimization.

Table 3– Design Variable Bounds for Optimization

Design Variable	Symbol	Range
Twist Location 1	r_1/R	$0.3 - 0.5$
Twist Location 2	r_2/R	$0.6 - 0.8$
Twist 1	θ_1	-60 deg – -30 deg

Twist 2	θ_2	-30 deg – -10 deg
Twist 3	θ_3	-20 deg – 0 deg
Taper Location 1	r_3/R	0.3 – 0.5
Taper Location 2	r_4/R	0.6 – 0.8
Taper 1	c_1	0.5 – 1.4
Taper 2	c_2	0.5 – 1.0
Taper 3	c_3	0.5 – 1.0

A. Pareto Front Convergence and Optimal Design Result

The surrogate-based optimization was performed over six update iterations using the Expected Improvement (EI) criterion to adaptively select new sample points. Each design point was evaluated using the free wake model, and the surrogate model was refined iteratively to improve prediction accuracy in promising regions of the design space. The process began with an initial dataset composed of 200 design points generated by Latin Hypercube Sampling (LHS) method, ensuring random sampling of the design space. Next, for each update iteration, 16 new sample points were added: 8 points were selected among the optimum data points, and the remaining 8 points were chosen by maximizing the EI criterion to promote exploration in uncertain areas of the model. This update strategy was repeated for 6 iterations, resulting in a final dataset containing 296 high-fidelity data points. This dataset formed the basis for the final Gaussian Process Regression (GPR) model used in performance prediction and design optimization.

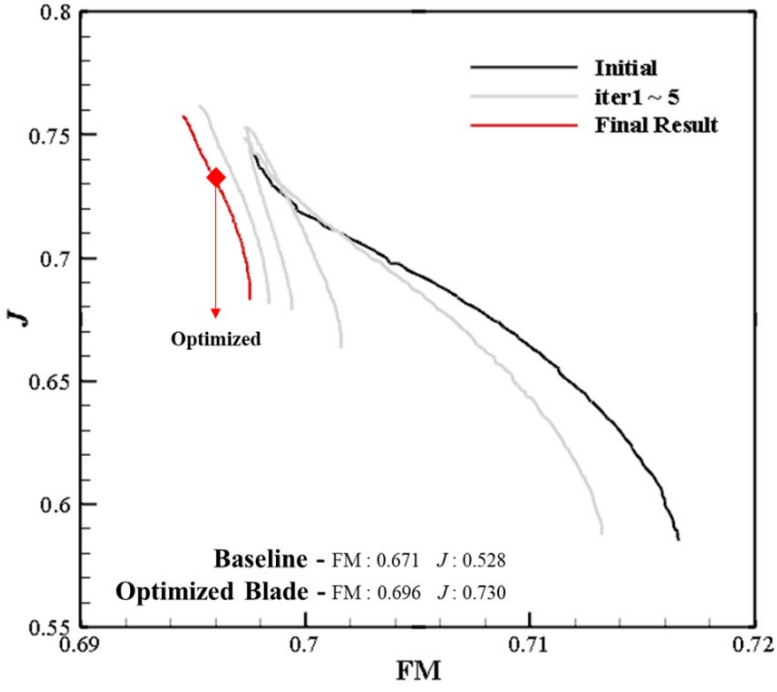

Fig. 5 – Pareto front history across optimization iterations

Fig. 5 shows the Pareto front of each iteration step. The black curve represents the initial pareto front obtained from the initial dataset, while the light gray curves show pareto fronts from iterations 1 through 5. The final pareto front, which is identical to the pareto front from iteration 5, suggests that the optimization process has converged. Among the final pareto front, an optimized blade design which shows better performance in both hover and forward flight was selected for further evaluation. The figure of merit of the optimized blade was 0.696 and the propulsive efficiency was 0.730, which corresponds to an improvement of approximately 3.7% in hover and 68.3% in forward flight.

Fig. 6 shows the twist and chord distributions of the baseline and optimized blade designs. The optimized twist distribution shows a more aggressive negative twist in the inboard region where $r/R < 0.5$ and less steep negative twist in the outboard region where $r/R > 0.7$. The twist distribution of the optimized blade is more similar to the hyperbolic twist distribution, which is an ideal twist distribution to minimize power consumption in hover [16]. Simultaneously, the chord distribution is more tapered in the optimized blade, especially beyond $r/R > 0.6$, resulting in reduced blade area and power consumption in the outer region. This geometry reflects a deliberate trade-off: boosting inboard lift and reducing tip vortex strength, both of which contribute to higher aerodynamic efficiency

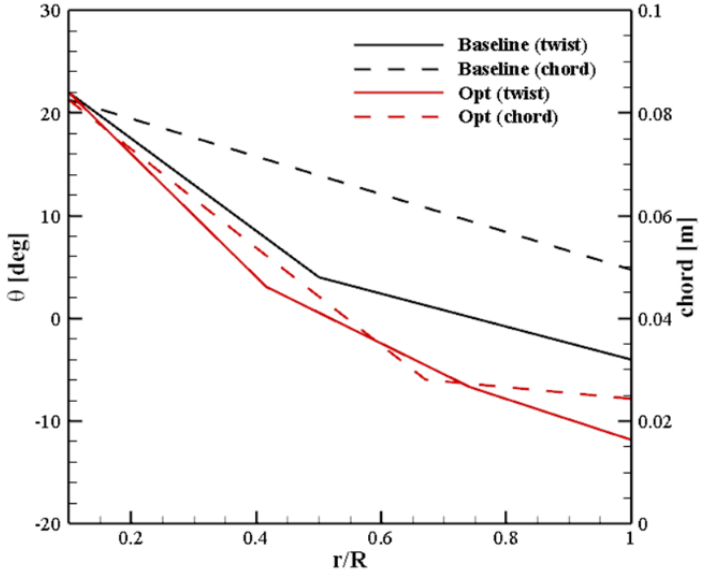

Fig. 6 – Twist and chord distributions between baseline and optimized blade

Fig. 7 shows the spanwise distribution of sectional thrust and power in hover. Compared to the baseline blade, the optimized blade generates higher thrust loading in the mid-span region where $0.3 < \mathrm{r/R} < 0.7$, where inflow conditions are favorable and induced velocity is lower. This shift redistributes the load away from the highly inefficient tip region. Similarly, the optimized blade generates higher power loading in the mid-span region and lower power loading in the outboard region.

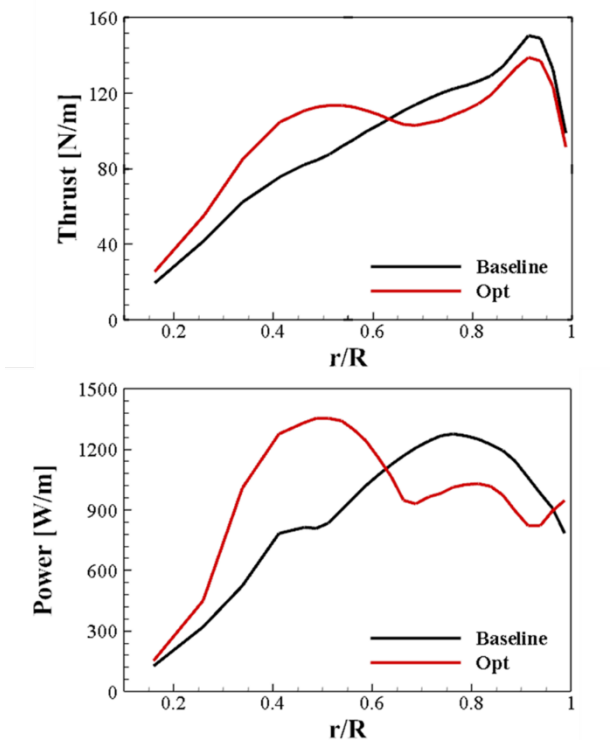

Fig. 7 – Thrust and power loading distributions in hover flight

The improved spanwise utilization directly contributes to the increased figure of merit. The combination of redistributed thrust and smoothed power consumption indicates that the optimized blade operates closer to ideal loading conditions, minimizing induced and profile losses during hover.

The aerodynamic performance in forward flight was also evaluated using spanwise thrust and power distributions, as shown in Fig. 8 and Fig. 9. In Fig. 8, the optimized blade shows higher thrust in the inboard region where $r/R < 0.5$. The redistributed twist and chord distribution of the optimized blade decreases the outboard thrust, thus increasing the thrust efficiency, which is consistent with the result from hover. Similarly, Fig. 9 confirms that energy consumption in the tip region is reduced, resulting in lower torque demand for a given thrust level. This redistribution leads to an improved thrust-to-power ratio, i.e., higher advance ratio J, without compromising overall thrust capability. The blade adapts more effectively to skewed inflow, a key advantage for tiltrotors operating at various flight attitudes.

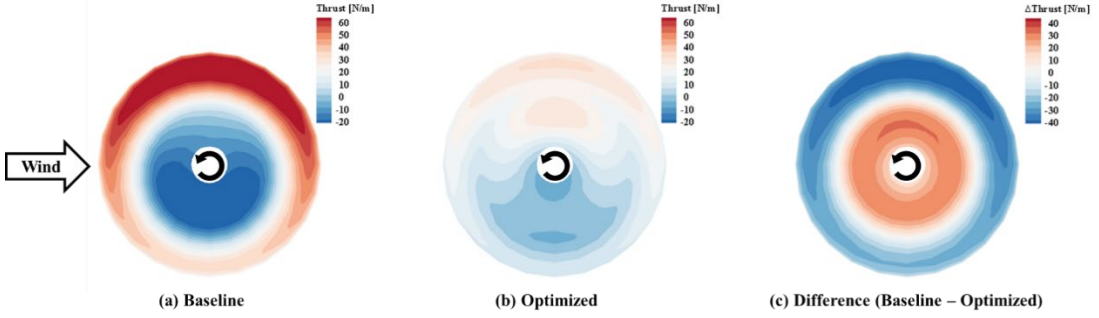

Fig. 8 – Spanwise thrust distribution in forward flight

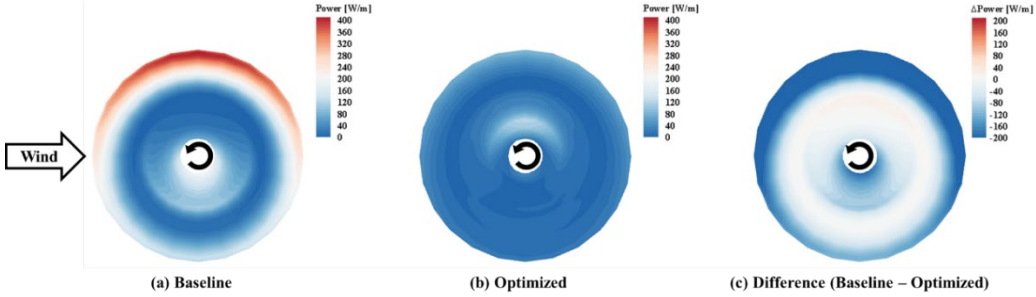

Fig. 9 – Spanwise power loading in forward flight

4. CONCLUSIONS

This study presented a surrogate-based aerodynamic optimization framework for the design of prop-rotor blades in quad-tiltrotor UAVs, with a particular focus on supporting the dual-mode operation—vertical takeoff and landing (VTOL) and efficient forward flight—of the QTP-UAV developed by KARI. To evaluate accurate rotor aerodynamics with efficiency, a Blade Element Method (BEM) coupled with a free wake model was employed. Each blade was modeled as a lifting line, and aerodynamic forces were computed for discrete spanwise elements using local inflow conditions derived from the induced velocity field from the convicted vortex filaments shed from blade trailing edges.

Using this aerodynamic solver, a Gaussian Process Regression (GPR) model was constructed as a surrogate model to predict the blade performance across the design space. In initial iteration, 200 data points for the design of experiment (DOE) was selected using Latin Hypercube Sampling (LHS) method, and then six update iterations were performed. In each update iteration, 16 new points were adaptively selected based on optimum convergence and expected improvement (EI) and therefore 296 designs are used to train the surrogate model. After update, the distribution of the pareto fronts are converged and the final pareto front revealed the trade-off relationship between hover and forward flight performance. Among the final pareto front, an optimum design was selected and the optimized blade exhibited a notable enhancement in both performance metrics compared to the baseline configuration: the figure of merit improved from 0.671 to 0.696, while the advance ratio increased from 0.528 to 0.730. In addition to performance improvements, detailed aerodynamic analyses were performed. The results revealed that the optimized blade planform yielded more favorable inflow distributions and reduced profile drag across the span.

Overall, this research illustrates the viability and effectiveness of integrating mid-fidelity aerodynamic models with probabilistic surrogate modeling for tiltrotor blade design. The framework offers a balanced trade-off between fidelity and efficiency, making it well-suited for iterative design processes, early-stage optimization, and system-level integration studies. Furthermore, the modular nature of the framework allows for future expansion into multidisciplinary domains—such as structural optimization, vibration analysis, and aeroacoustics performance—by incorporating corresponding simulation data into the surrogate model. Future work will focus on extending the current framework to incorporate robustness under off-design conditions with broader flight envelope. Additionally, coupling the surrogate model with real-time trajectory optimization or control system design could further enhance the autonomy and mission effectiveness of UAV platforms like the QTP-UAV. The techniques demonstrated here lay a strong foundation for the data-driven, simulation-informed design of next-generation rotorcraft systems.

REFERENCES

[1] S. Jung and H. Kim, "Analysis of Amazon Prime Air UAV Delivery Service", *Journal of Knowledge Information Technology and Systems*, Vol. **12**, No. 2, 2017, pp. 253–266.

[2] S. M. Shavarani, M. G. Nejad, F. Rismanchian and G. Izbirak, "Application of hierarchical facility location problem for optimization of a drone delivery system: a case study of Amazon Prime Air in the city of San Francisco", *The International Journal of Advanced Manufacturing Technology*, Vol. **95**, 2018, pp. 3141–3153.

[3] L. Vempati, R. Crapanzano, C. Woodyard and C. Trunkhill, "Linear Program and Simulation Model for Aerial Package Delivery: A Case Study of Amazon Prime Air in Phoenix, AZ", *17th AIAA Aviation Technology, Integration, and Operations Conference*, 2017.

[4] A. Misra, S. Jayachandran, S. Kenche, A. Katoch, A. Suresh, E. Gundabattini, S, K, Selvaraj and A. A. Legesse, "A Review on Vertical Take-Off and Landing (VTOL) Tilt-Rotor Unmanned Aerial Vehicles", *International Journal of Aerospace Engineering*, Vol. **2022**, 2022, pp. 1–16.

[5] M. Imiela, "High-fidelity optimization framework for helicopter rotors", *Aerospace Science and Technology*, Vol. **23**, 2012, pp. 2–16.

[6] S. W. Choi and J. M. Kim, "Investigation into the Aerodynamic Performance of the Tiltrotor Unmanned Aerial Vehicle Proprotor", *Journal of Aircraft*, Vol. **50**, No. 6, 2013, pp. 1756–1763.

[7] W. Johnson, "Airloads and Wake Geometry Calculations for an Isolated Tiltrotor Model in a Wind Tunnel", *27th European Rotorcraft Forum*, Moscow, Russia, Sep. 2001.

[8] G. Wilke, "Variable-Fidelity Methodology for the Aerodynamic Optimization of Helicopter Rotors", *AIAA Journal*, Vol. **57**, No. 8, 2019, pp. 3145–3158.

[9] J. B. Lee, J. W. Lee, K. J. Yee, S. J. Oh and D. K. Kim, "Development of an Aerodynamic Performance Analysis Module for Rotorcraft Comprehensive Analysis Code", *Journal of The Korean Society for Aeronautical and Space Sciences*, Vol. **37**, 2009, pp. 224**–**231.

[10] J. L. Walsh, K. C. Young, J. I. Pritchart, H. M. Adelman and W. R. Mantay, "Integrated Aerodynamic/Dynamic/Structural Optimization of Helicopter Rotor Blades Using Multilevel Decomposition", NASA Technical Paper 3465, Jan. 1995.

[11] J. W. Lim, "Consideration of structural constraints in passive rotor blade design for improved performance", *The Aeronautical Journal*, Vol. **119**, No. 1222, 2015, pp. 1513–1539.

[12] D. Lee, Y. Kang, D. Kim and K. Yee, "Aeroelastic Design and Comprehensive Analysis of Composite Rotor Blades Through Cluster-Based Kriging", *AIAA Journal*, Vol. **60**, No. 10, 2022, pp. 5984–6004. 15

[13] B. Glaz, P. Friedmann and L. Liu, "Surrogate based Optimization of a Helicopter Rotor Blade for Vibration Reduction in Forward Flight", *Structural and Multidisciplinary Optimization*, Vol. **35**, 2008, pp. 341–363. https://doi.org/10.1007/s00158- 007-0137-z.

[14] H. J. Kang, "Design Optimization of QTP-UAV Prop-Rotor Blade Using ModelCenter", *Journal of Aerospace System Engineering*, Vol. **11**, No. 4, 2017, pp. 36–43.

[15] J. G. Leishman, *"Principles of Helicopter Aerodynamics*", Cambridge University Press, 2016.

[16] J. G. Leishman, M. J. Bhagwat and A. Bagai, "Free-Vortex Filament Methods for the Analysis of Helicopter Rotor Wakes", *Journal of Aircraft*, Vol. **39**, No. 5, 2002.